PRAMANA
— journal of
physics

Vol. 81, No. 2
August 2013
pp. 319–330

Effect of doping and annealing on the physical properties of ZnO:Mg nanoparticles

SABER FARJAMI SHAYESTEH* and ARMIN AHMADI DIZGAH
Nanostructure Laboratory, Department of Physics, University of Guilan, Guilan, Iran
*Corresponding author. E-mail: saber@guilan.ac.ir

MS received 17 October 2012; revised 6 April 2013; accepted 6 April 2013

Abstract. Well-dispersed undoped and Mg-doped ZnO nanoparticles with different doping concentrations at various annealing temperatures are synthesized using basic chemical solution method without any capping agent. To understand the effect of Mg doping and heat treatment on the structure and optical response of the prepared nanoparticles, the samples are characterized using X-ray diffraction (XRD), energy-dispersive X-ray (EDX), UV–Vis optical absorption, photoluminescence (PL), scanning electron microscopy (SEM) and transmission electron microscopy (TEM) measurements. The UV–Vis absorbance and PL emission show a blue shift with increasing Mg doping concentration with respect to bulk value. UV–Vis spectroscopy is also used to calculate the band-gap energy of nanoparticles. X-ray diffraction results clearly show that the Mg-doped nanoparticles have hexagonal phase similar to ZnO nanoparticles. TEM image as well as XRD study confirm the estimated average size of the samples to be between 6 and 12 nm. Furthermore, it is seen that there was an increase in the grain size of the particles when the annealing temperature is increased.

Keywords. ZnO:Mg nanoparticles; annealing; doping; structure; optical response.

PACS Nos 78.67.Bf; 78.55.Et

1. Introduction

Semiconductor nanoparticles show unique, size-dependent optical properties due to the quantum confinement effect. The ZnO and its compositions are found to be useful in optoelectronic applications and many other applications such as gas sensors, chemical sensors, solar cells, biomedical devices and photocatalysts due to their wide band-gap potential (3.3 eV) [1,2]. Various methods such as the sol–gel [3], precipitation [4,5], microwave [6] spray pyrolysis [7] and thermal evaporation [8] methods were reported for preparing nanosize ZnO. In most of these methods, various capping agents are used to prevent the growth of particles with time.

One of the major challenges in optimizing the optical properties of ZnO is the incorporation of doping ions into the ZnO lattice. Doping with selective elements offers an

DOI: 10.1007/s12043-013-0562-z; ***e*Publication: 26 July 2013**

effective method to enhance and control the structural, electrical and optical properties of ZnO nanoparticles. ZnO doped with proper elements, such as Al, Mn, Cd, Mg, Ni and Cr, has been studied [9,10]. By doping with a wider band-gap material [11], the band gap of ZnO particles can be tuned for manufacturing light-emitting devices operating in a wider wavelength region. The doping of ZnO with a metal (Al, Cu, Fe, Ni, Co) can change its properties. ZnO is an ideal material for UV emission; but the intensity of UV emission is weak. However, doping with Group II elements (Cd, Mg) may modulate the value of the band gap and increase the intensity of UV emission [12].

Mg-doped ZnO nanostructures are very interesting owing to their unique optical and electrical properties and more work is in progress to control the physical properties of doped ZnO particles systematically. Therefore, a suitable method for preparing doped ZnO with less operating cost, less synthesis time, narrow size range and better properties is a challenge for scientists.

Hence, in this work, we present a simple and low-cost chemical method for synthesizing monodisperse Mg-doped ZnO nanoparticles with semispherical shape, without using a surfactant. Also, we investigate the effect of magnesium doping and annealing on the structural and optical properties of ZnO nanoparticles.

2. Experimental details

2.1 *Materials and synthesis procedure*

ZnO:Mg nanoparticles were prepared by chemical method as follows: 0.002 M zinc acetate ($Zn(CH_3COO)_2{\cdot}2H_2O$, 99%, Merck) and 0.005 M sodium hydroxide were dissolved in 10 ml ethanol. The solution was refluxed for 90 min at 80°C keeping the temperature and speed of the magnetic stirrer constant. The NaOH should be added slowly and dropwise with continuous stirring to zinc acetate solution to control the pH and rate of reaction due to the common ion effect. Magnesium acetate ($Mg(CH_3OO)_2{\cdot}4H_2O$, 99%, Merck) dissolved in ethanol was added to the above solution to produce Mg-doped samples with 0–10% atomic percentage. For increasing the precipitation speed and controlling the agglomeration, the solution was put in ice bath. In order to remove Na^+ ions and CH_3O^- ions, nanoparticles of heptane were added to the solution. Then, the prepared nanoparticles were rapidly washed with distilled water and acetone to remove the ions and insoluble materials remaining in the product. Finally, the washed particles were dried at 100°C for 24 h.

2.2 *Characterization methods*

X-ray diffraction (XRD) was done with a Philips PW3710 diffractometer using Cu K_α radiation source with 1.5418 Å wavelength. The photoluminescence (PL) measurements were performed using an Avantes 2048-TEC PL spectrometer and samples were excited by employing 325 nm wavelength from Xe-lamp source. The images of nanoparticles were observed using Philips CM10 transmission electron microscope (TEM) and energy-dispersive X-ray (EDX) spectroscopy was done using a Philips X130 spectrometer. EDX samples were prepared by suspending the nanoparticles in ethanol and dispersing them on copper grids.

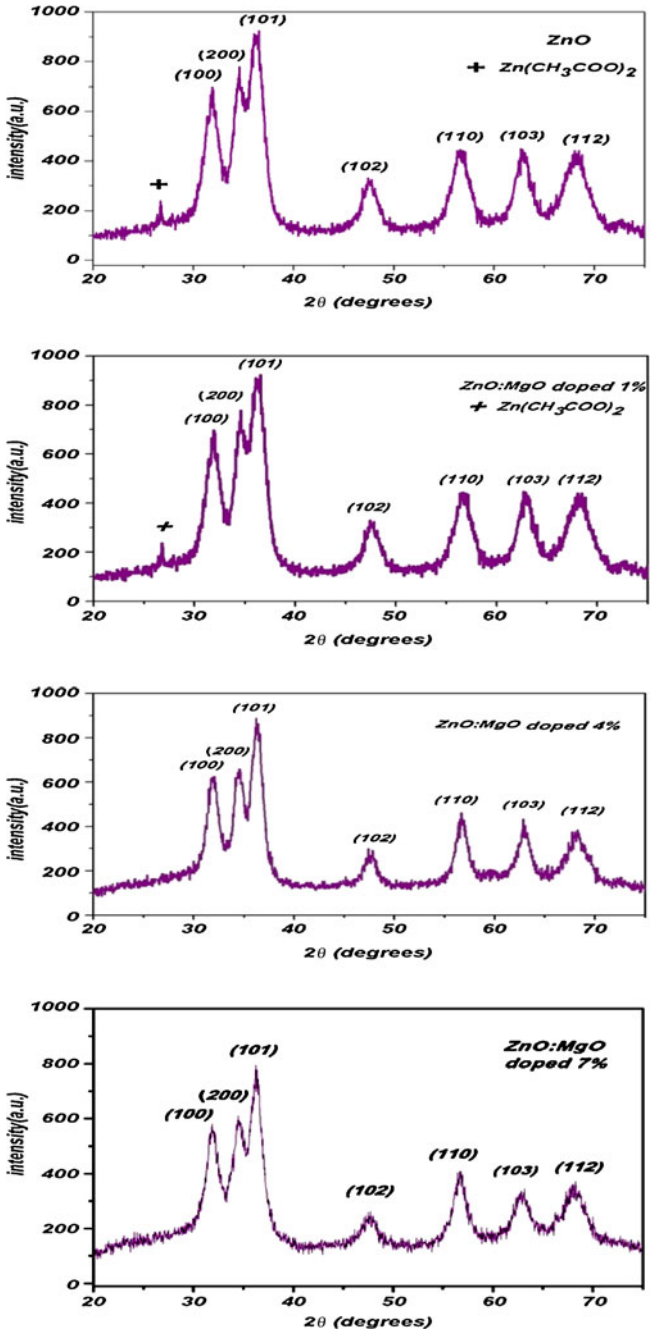

Figure 1. X-ray diffraction pattern of ZnO nanoparticles doped with different Mg concentrations. The XRD peaks can be indexed to hexagonal phase structure.

3. Results and discussion

Figure 1 presents XRD spectra of ZnO nanoparticles doped with various Mg doping concentrations. There are seven broad peaks corresponding to (1 0 0), (2 0 0), (1 0 1), (1 0 2), (1 1 0), (1 0 3) and (1 1 2) which have been indexed to the standard pattern of hexagonal ZnO. No second phase is within the limit of the XRD measurement and apparently there is no peak for MgO. There is a weak peak at about 28° which can be due to $Zn(CH_3COO)_2$ and with increasing doping concentration it disappears. Therefore, the XRD pattern indicating Mg ions are substituted for Zn ions because both have very similar ionic radii (0.57 and 0.60 Å), and there are no variation in the structure of the ZnO nanoparticles.

The average size of the crystallite (L) was calculated from the full-width at half-maximum (FWHM) of the (1 0 1) peak using the Debye–Scherrer formula [13] (ignoring the effect of strain):

$$\beta_{\text{Total}} = \frac{k\lambda}{L\cos\theta}, \tag{1}$$

where θ is the Bragg angle, λ is the radiation wavelength and k is a constant which depends on the peak shapes, crystallite habit and particle shape. The average diameter of particles was calculated by Williamson–Hall method [14]. In this method, there are two sources for the broadening of diffraction peaks: crystallite sizes and inhomogeneous strain (due to homogeneous strain peaks shifted). By using eqs (1) and (3)

$$\beta_{\text{Total}} = \beta_{\text{Lattice}} + \beta_{\text{Strain}} = c\varepsilon\tan\theta + \frac{k\lambda}{L\cos\theta} \tag{2}$$

$$\cos\theta\beta_{\text{Total}} = c\varepsilon\sin\theta + \frac{k\lambda}{L} \tag{3}$$

and drawing $\cos\theta\beta_{\text{Total}}$–$\sin\theta$ plot which has a straight line form ($y = ax + b$), strain and crystallite size can be calculated by obtaining the slope and y-intercept of the depicted line, respectively.

The estimated particle sizes of samples with different Mg concentrations are given in table 1. The particle size is gradually decreased with increasing Mg doping. As the Mg

Table 1. The average crystallite size of Mg-doped ZnO sample calculated from XRD.

Mg doping concentration (%)	Average crystallite size (nm)
0.0 (undoped)	13.0
1	11.0
4	9.4
7	7.6
10	6.3

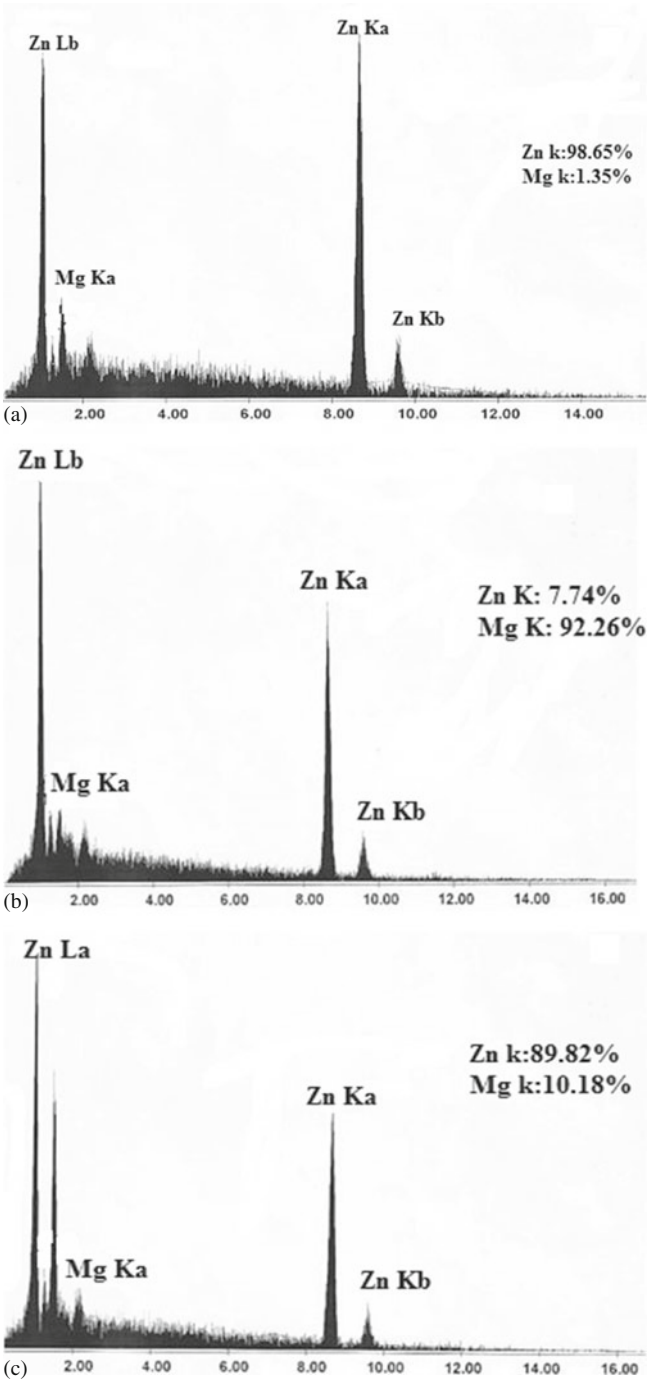

Figure 2. EDX spectra of ZnO nanoparticles doped with (**a**) 4%, (**b**) 7% and (**c**) 10% Mg concentrations. Samples were annealed at 200°C.

concentration increases, the optical band gap also increases because of the replacement of Mg with Zn in the crystal lattice (MgO has a higher band gap (7.8 eV) than that of ZnO (3.4 eV)). Also, the XRD patterns of Mg-doped ZnO samples show a slight shifting of the centre of diffraction peaks toward higher angle compared to pure ZnO [15].

The shifts of the peak indicate a compaction of the unit cell, possibly, because the Mg ions prefer to occupy the interstitial sites. Such a change is expected, because the Mg ion has smaller ionic radius compared to Zn ion [16]. The pure phase of the XRD and the slight shift of the peak position imply that the Mg atoms effectively occupy the ZnO lattices.

The Mg incorporation and percentage of Mg in doped ZnO samples were analysed by energy-dispersive X-ray (EDX) spectroscopy (figure 2). It seems that in most cases the EDX may have overestimated the actual Mg in the samples.

Figure 3a shows the UV–Vis absorption spectra of ZnO nanoparticles as a function of wavelength in the wavelength range from 200 to 600 nm at various annealing temperatures. By comparing the absorption position of the spectra, a blue-shift can be seen along with variation of annealing temperatures which agree with the reported experimental results [17,18]. All annealed ZnO nanoparticles show stronger UV–Vis absorbance than the as-grown ZnO nanoparticles. Also, the direct band-gap energy of the prepared nanoparticles is estimated by extrapolating the straight line plot of $(\alpha h\upsilon)^2$ vs. the photon energy ($h\upsilon$) [19] (figure 3b). As shown in figure 3, with increasing annealing temperatures, optical band gap decreases. This decrease in band-gap energy is in good agreement with the corresponding blue-shift seen in the absorption edge mentioned above. The band gap of ZnO particles is a function of size under effective mass approximation (EMA) as well as under tight binding approximation.

Figure 4 shows the UV–Vis absorption spectra of Mg-doped ZnO nanoparticles with various Mg concentrations at different annealing temperatures. It is found that when annealing temperature increases, the energy gap decreases. The decrease in gap energy may be due to increase in size of the nanoparticles. Also, with increase in doping concentration, the gap energy increases and size of the particles decreases as shown in figure 4.

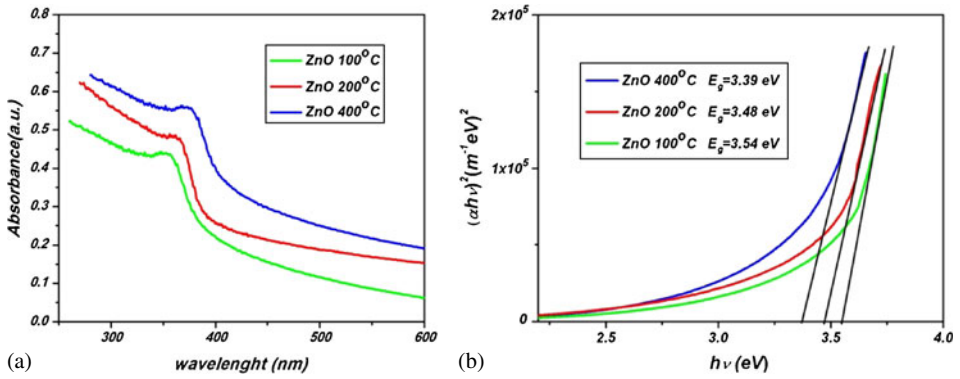

Figure 3. (**a**) Absorption spectra of ZnO nanoparticles at different annealing temperatures and (**b**) $(\alpha h\upsilon)^2$ vs. $h\upsilon$.

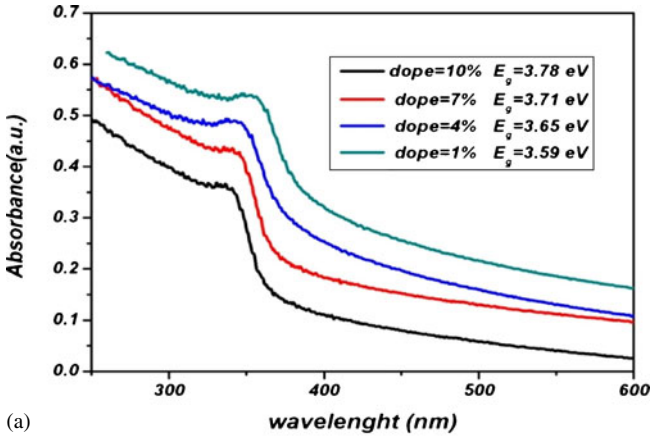

(a)

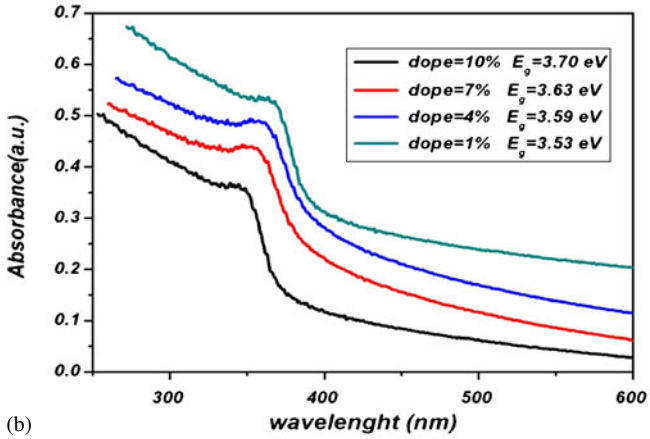

(b)

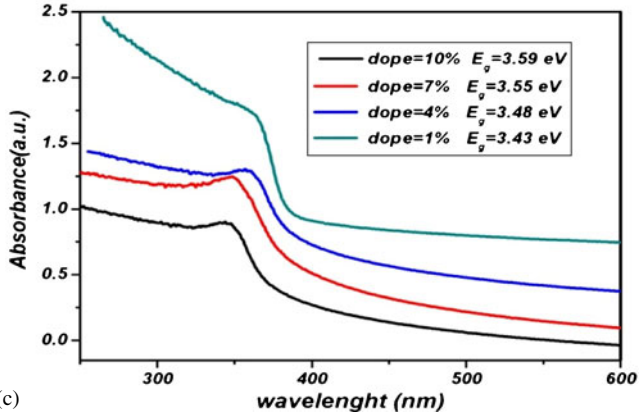

(c)

Figure 4. UV–Vis absorption spectra of ZnO nanoparticles doped with different Mg concentrations at various annealing temperatures: (**a**) 100°C, (**b**) 200°C and (**c**) 400°C.

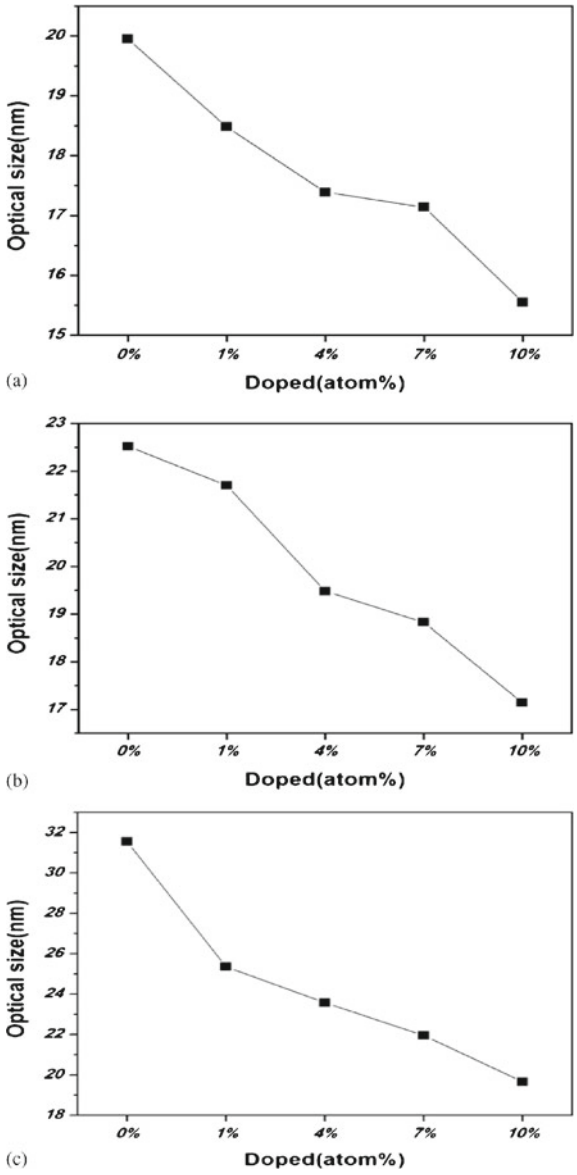

Figure 5. Size of ZnO for various Mg doping concentrations at different annealing temperatures: (**a**) 100°C, (**b**) 200°C and (**c**) 400°C.

This result is associated not only with the grains growing more easily when the temperature is higher, but also with Mg dopant. The change in the band gap can be due to quantum confinement effects. The band gap is proportional to the inverse size of the nanoparticles, and the band gap of the nanoparticles is slightly bigger than that of the bulk materials. It

is important that the Mg doping can widen the band gap of ZnO nanoparticles, a result that has been reported in many reports on Mg-doped ZnO films or other nanomaterials (nanowires or nanorods) [20–22].

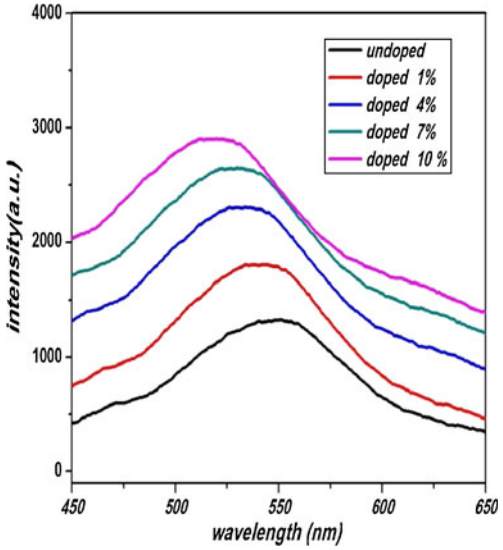

Figure 6. PL spectra of ZnO nanoparticles with different doping concentrations at 100°C. Excitation wavelength is 320 nm.

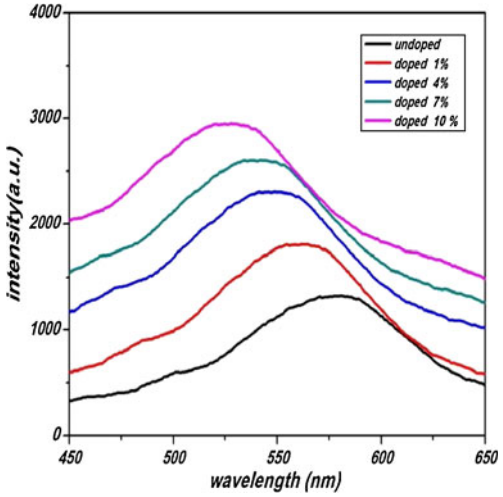

Figure 7. Effect of ageing on the PL spectra of a few selected ZnO nanoparticles with different doping concentrations at 100°C.

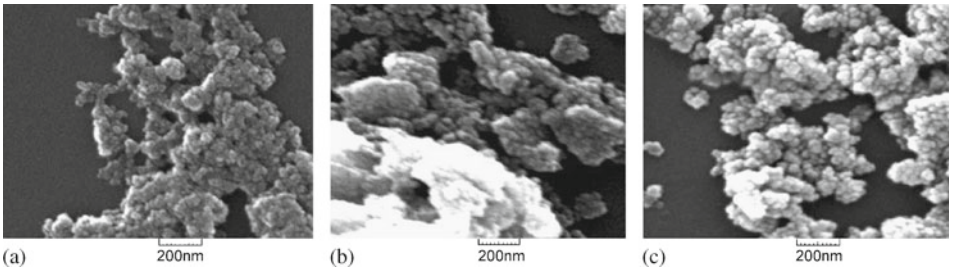

Figure 8. SEM images of ZnO annealed at different temperatures: (**a**) 100°C, (**b**) 200°C and (**c**) 400°C.

The estimated size of the ZnO nanoparticles as a function of Mg doping concentration at different annealing temperatures (100°C, 200°C and 400°C) is depicted in figure 5. It is clear that the size of the particles decreases with increasing doping concentration and the size increases with annealing temperature as expected from XRD results.

The room-temperature PL spectra of Mg-doped ZnO nanoparticles excited at 320 nm are shown in figure 6. All the samples show a broad green band with a blue-shift by increasing Mg doping concentration compared to the emission peak of the undoped sample. The green emission involves transition from the band edge (or shallow level close to band) to a defect level. This emission can be due to oxygen interstitials [23–25].

To investigate the effect of ageing on the emission properties, the PL spectra of the as-prepared and Mg-doped ZnO after 90 days is depicted in figure 7. As shown in figure 7, green emission peak of the samples shift towards higher wavelength (red-shift) compared to figure 6 due to ageing [25]. This shift can be due to increase in size of the particles and decrease in gap energy. However, with increasing doping concentration, amount of blue-shift of emission band (figure 6) decreases compared to fresh samples (figure 7) with respect to bulk ZnO which can arise from variation of surface levels and defect levels.

Scanning electron microscopy was employed to investigate the morphology of the samples. SEM micrographs of the as-prepared ZnO nanoparticles annealed at different temperatures are shown in figures 8a–c. Averages size of particles increases with increasing annealing temperatures. As seen in figure 8, the spherical particles can be distinguished in the pictures, though not very clearly and some clusters can also be found.

The TEM micrograph of the ZnO nanoparticles with different Mg doping concentration is presented in figure 9. As shown in figure 9, most of the particles are quasispherical and the size distribution histograms are also depicted. TEM picture (figure 9a-2) reveals that the size of the ZnO particle is about 12 nm with a narrow size distribution. The average size of the Mg-doped ZnO nanoparticles decreases as the Mg concentration increases.

4. Conclusions

The effect of Mg doping on the microstructure and optical properties of ZnO nanoparticles prepared by chemical method without using any capping agent has been investigated. The Mg substitution in the sample is indicated by EDX technique. The XRD patterns show that Mg-doped nanoparticles have hexagonal structure as that of ZnO and Mg substitution

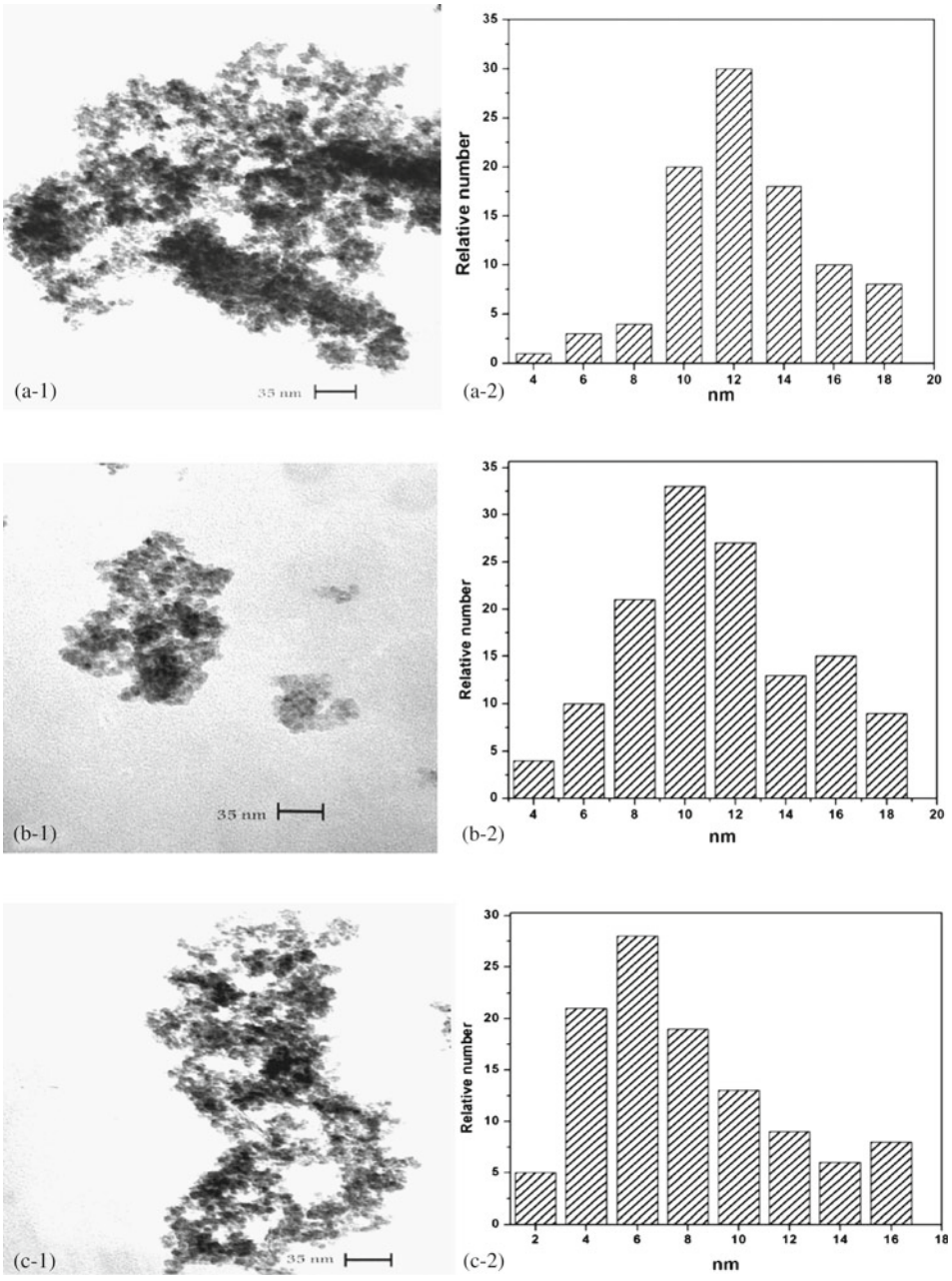

Figure 9. TEM spectra and particles size histogram of ZnO nanoparticles doped with (**a**) 0% Mg, (**b**) 4% Mg and (**c**) 10% Mg, annealed at 100°C.

affects the lattice volume very slightly. XRD, UV–Vis and PL measurements indicate that Mg substitute into ZnO lattice at Zn sites, instead of forming impurity compound or magnesium oxide. The crystallite sizes reduces due to the incorporation of Mg, while the band

gap increases. The estimated diameter of the nanoparticles found from the TEM well is consistent with the XRD results. The PL emission shows a blue-shift with increasing Mg doping concentration. Also, the green emission peak of the ageing samples shifts towards lower wavelength compared to fresh samples. The ultraviolet emission peaks blue-shift with an increase in the Mg doping concentration. The blue-shift observed in the UV–Vis spectrum is a typical signature of size confinement in ZnO nanoparticles.

Acknowledgement

The authors would like to acknowledge the financial support from the University of Guilan.

References

[1] Z Ling, C Leoch and R Freer, *J. Eur. Ceram. Soc.* **21**, 1977 (2001)
[2] C Y Hsu, T F Ku and Y M Huang, *J. Eur. Ceram. Soc.* **28**, 3065 (2008)
[3] F Mikara Juddin, K Iskandar and F G Okuyama, *J. Appl. Phys.* **89**, 6431 (2001)
[4] J H Kim, W C Choi, H Y Kim and Y Park, *J. Sol-Jel Sci. Technol.* **23**, 547 (2003)
[5] R Y Hong, J H Li, L Chen, D Q Liu, Y Zhenj and J Ding, *Powder Technol.* **189**, 246 (2009)
[6] S Kamarnen, M Bruno and M Mariani, *Mater. Res. Bull.* **35**, 1843 (2000)
[7] T Tani, L Madler and S E Pratsinis, *J. Nanopart. Res.* **4**, 337 (2002)
[8] Z R Dia, Z W Pan and Z L Wang, *Adv. Funct. Mater.* **13**, 9 (2003)
[9] Y Liu, J H Yang, Q F Guan, L L Yang, Y J Zhang, Y X Wang, B Feng, J Cao, X Y Liu, Y T Yang and M B Wei, *J. Alloys Compounds* **486**, 835 (2009)
[10] J Wang, W Chen and M R Wang, *J. Alloys Compounds* **449**, 44 (2008)
[11] L Kumari, W Z Li, Charles H Vannoy, Roger M Leblanc and D Z Wang, *Ceram. Int.* **35**, 3355 (2009)
[12] A Ohotomo *et al*, *Appl Phys. Lett.* **72**, 2466 (1998)
[13] B D Cullity and S R Stock, *Elementary of X-ray diffraction*, 3rd edn. (Prentice-Hall, Englewood Cliffs, New Jersey, 2001)
[14] G K Williamson and W Hall, *Acta Metall.* **1**, 22 (1953)
[15] K Matsumura, A Ohnishi, M Sasaki, T Kakuta and M Skamoto, *Appl. Phys.* Part 1 **46**, 1432 (2007)
[16] O Ohtono, M Kawasaki, T Koida, K Masabuchi, H Koinuma, Y Sakurai and Y Yoshida, *Appl. Phys. Lett.* **72**, 2466 (1998)
[17] Y X Liu, Y C Liu, D Z Shen, G Z Zhong, X W Fan, X G Kang, R Mu and D O Henderson, *Solid State Commun.* **121**, 531 (2002)
[18] V Noack and A Eychmuller, *Chem. Mater.* **14**, 1411 (2002)
[19] J I Pankove, *Optical process in semiconductors* (Prentice-Hall, New Jersey, 1971)
[20] A Ohtomo, K Tamura, M Kawasaki, T Makino, Y Segawa, Z K Tang, G Wong, Y Matsumoto and H Koinuma, *Appl. Phys. Lett.* **77**, 2204 (2002)
[21] H C Hsu, C Y Wu, H M Cheng, Z Y Wang, J W Zhao and L D Zhang, *Appl. Phys. Lett.* **89**, 013101 (2006)
[22] Y W Heo, M Kaufman and K Pruessner, *Solid-State Electron.* **47**, 2269 (2003)
[23] H S Kang, J W Kim and S Y Lee, *J. Appl. Phys.* **95**, 1246 (2004)
[24] A J Monteiro, M C Carno, M J Soures and T Wang, *J. Appl. Phys.* **98**, 013502 (2005)
[25] S Farjami Shayesteh and A Ahmadi Dizgah, *International Conference on Enabling Science and Nanotechnology* (Johor, Malaysia, 2012), DOI:10.1109/ESciNano.2012.6149677